

## Dynamics and Heating of Chromospheres

Wolfgang Kalkofen

*Harvard-Smithsonian Center for Astrophysics,  
60 Garden Street, Cambridge, MA 02138, USA*

**Abstract.** Heating and dynamics of the solar as well as stellar chromospheres are separate phenomena, judging by their spatial and temporal characteristics in the Sun. Simulations of chromospheric heating in late-type stars as well as simulations of the dynamics of the large-amplitude oscillations of internetwork calcium bright points in the solar atmosphere reproduce the main features of the respective phenomena. Differences between models and observations imply (1) that the Sun has a permanent, hot chromosphere and that its temperature structure cannot be obtained by averaging the time-dependent temperature profile of a model that describes only the oscillations, and (2) that the acoustic waves causing the dynamics and the heating propagate upward as spherical waves.

### 1. Introduction

The quiet solar chromosphere is bifurcated into magnetic network on the boundary of supergranulation cells (CB) and internetwork chromosphere in the cell interior (CI). The CI is largely free of magnetic fields strong enough to be dynamically important. As a consequence, only acoustic waves play a role in the heating and large-amplitude dynamics of the internetwork chromosphere, at least below the so-called magnetic canopy.

The internetwork chromosphere shows two important processes involving acoustic waves: large-amplitude oscillations with a period of about 3 min at a small number of discrete locations, and heating throughout the chromosphere. Observations imply that the two phenomena are unrelated, but theorists have linked them, based on the plausible argument that since both involve 3 min waves as well as heating they must belong to the same process. This paper examines the proposition that chromospheric heating and the 3 min oscillations as seen in calcium bright points (also called grains, or  $K_{2v}$  or  $H_{2v}$  bright points) are merely two aspects of the same phenomenon, by confronting model predictions with observations. The emphasis is mainly on the time-dependent model of Carlsson & Stein (1994, 1995; hereafter collectively CS) since it linked oscillations and heating most directly by constructing the model for the time-average temperature structure of the internetwork chromosphere from their time-dependent, dynamical model, and since the simulations of the dynamics are based on an observed photospheric velocity spectrum and should therefore afford a quantitative comparison with observations.

In Section 2 we review the spatial and temporal characteristics of 3 min oscillations, in Section 3 we estimate the contribution of 3 min oscillations to chromospheric heating, in Section 4 we consider the geometry of wave propagation in the chromosphere and in Section 5 we compare predictions of the Ca II and Mg II emissions for late-type stars with observations; in Section 6 we draw conclusions.

## 2. Spatial and temporal characteristics of grains

In the absence of magnetic fields only acoustic waves are allowed in the purely upward direction. They produce oscillations near the acoustic cutoff period of  $P_c = 3$  min (corresponding to a frequency of  $\nu_c = 5$  mHz). Oscillations of large amplitude, which are the subject of the wave simulations by Carlsson & Stein, result in bright regions that are visible at all heights in the internetwork chromosphere. In the middle chromosphere where they are called  $K_{2v}$  and  $H_{2v}$  grains they appear at a small number of discrete and largely fixed locations. In contrast, 3 min oscillations of low amplitude are seen everywhere.

The density of  $K_{2v}$  bright points has been measured by Brandt et al. (1992) who find 10 to 20 in a typical supergranulation cell. Their diameter is about 2 Mm (for  $H_{2v}$  bright points, Cram & Damé 1983) and their filling factor  $f \sim 5\% - 10\%$  (v.Uexküll & Kneer 1995; hereafter vUK95); for a diameter of  $\sim 30$  Mm of a typical supergranulation cell, these data imply again the observed density of bright points.

Calcium grains occupy more-or-less fixed locations in the internetwork chromosphere. Figure 2 of Lites, Rutten & Kalkofen (1993; hereafter LRK93) shows the intensity of the H line of Ca II as a function of wavelength and time at a fixed position. The blue emission peak,  $H_{2v}$ , left of the dark line center, brightens with a typical temporal separation of 3 min, but there are longer periods without strong oscillatory activity, amounting to a temporal filling factor of about 50%. It is noteworthy that the grain remains fixed at the same location for the duration of the 1 h observing run. This is found to be a general property of grains, as shown also in the observations of Damé (1984), where the cumulative filling factor of grains after 1 h is still much less than unity although for random locations a nearly complete coverage of the CI would be expected. This behavior contradicts the notion of Rutten & Uitenbroek (1991) and of vUK95 who have suggested that grains appear at random in space and time.

## 3. Heating from 3 min oscillations

Figure 1 shows the intensity at 11 positions in the internetwork chromosphere with simultaneous maximal brightening, in a 1 h observing run of vUK95. The intensity in a 300 mÅ band centered on  $K_{2v}$  is normalized to the intensity average over the whole CI. The authors define a bright point by an intensity enhancement of at least 50%. A typical enhancement is by 60%. The intensity peaks are separated by approximately 3 min and a wave train lasts 3 to 5 wave periods. It is interesting that the background oscillates also with a period of about 3 min, but with distinctly lower amplitude, reaching typically  $\pm 10\%$ , with

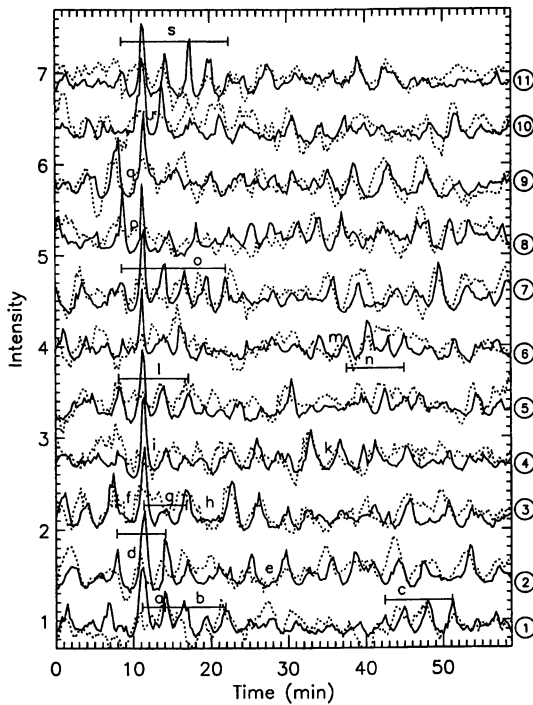


Figure 1. K line intensity with a  $300 \text{ m}\text{\AA}$   $K_{2v}$  filter (vUK95)

more or less symmetrical profiles, whereas the strong bright-point oscillations are asymmetric.

The intensity profiles of Fig. 1 allow us to estimate the contribution made by dissipation in the bright-point oscillations to chromospheric heating. Since heat conduction is negligible in the chromosphere and waves are the only means of energy transport, the emission measures directly the local heating.

A typical maximal intensity enhancement above the background is by 60% and the width of the profile amounts to about one third the wave period. Taking into account the approximately triangular shape of the intensity profile and a temporal intermittence of 50%, the fractional emission due to large-amplitude 3 min oscillations is about 5%.

The amplitude of the intensity and the duration of the excess emission are affected by the  $300 \text{ m}\text{\AA}$  filter centered on the  $K_{2v}$  emission peak since the radiation is emitted over a considerable height range. An intensity profile obtained with a spectrograph gives greater intensity enhancement but for a shorter duration. Thus, the H line observed by Kariyappa (1992) shows an  $H_{2v}$  intensity increase by a factor of 2.7 and a decay time of about 5% of the wave period. The fractional emission estimated in that case is the same as with the data taken with the filter, which indicates that the fractional heating caused by the wave is not strongly height dependent.

The total contribution made by bright-point oscillations to heating in the internetwork chromosphere must take into account that 90% to 95% of the area are heated only by the background process and are without large-amplitude

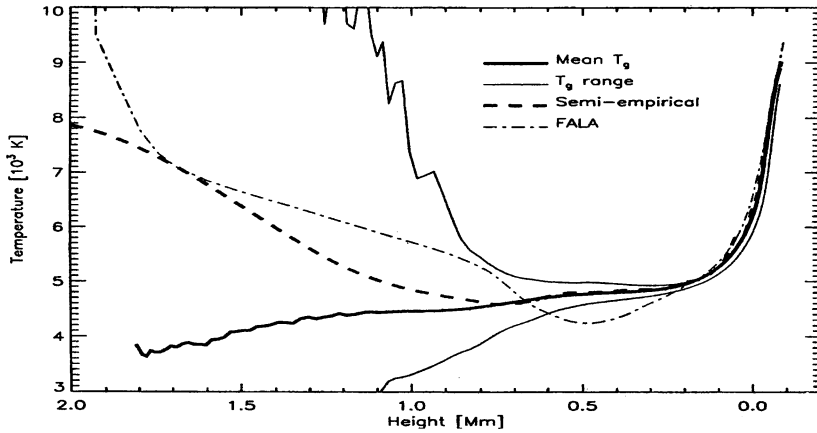


Figure 2. Kinetic, average and empirical temperatures of chromospheric models (from CS)

oscillations. Overall heating of the chromosphere due to dissipation in the oscillations is therefore reduced and amounts to heating above the background by only a few tenths of one percent.

Figure 2 shows various temperatures from the Carlsson & Stein simulations. The two bounding curves give the range of variation of the kinetic temperature based on velocity measurements in a photospheric Fe I line by LRK93, the heavy drawn curve is the time-average temperature of the time-dependent model, the dashed curve represents the time-independent model that is constructed so as to match the time average emission of the time-dependent model, and the dash-dot curve is the coolest of the empirical models of the series of models by Fontenla, Avrett & Loeser (1993; hereafter FAL), labeled FALA in the figure.

Since the temperature structure of the CS model is determined such that the emission due to the time-averaged dissipation in the oscillations is equal to the emission in the so-called semiempirical model, the ratio of the emission during the oscillation to the emission of the semiempirical model is unity. Since the vUK95 observations show this ratio to be a few percent it is clear that the CS model lacks the background emission of the solar chromosphere.

While the CS model (the dashed curve in Fig. 2) is too cool to reproduce the total emission of the solar chromosphere (the dash-dotted curve), it is too hot to reproduce only the emission due to the 3 min wave.

We can estimate the difference of the emission of the CS model from that of the FAL model by comparing the Planck functions for the Ca II lines at the height of 1 Mm, noting that in a steady chromospheric model (as FALA and CS), the line source function agrees with the Planck function up to the height of formation of the H<sub>2</sub> and K<sub>2</sub> emission peaks; at greater height, the source function drops monotonically with height, accounting for the absorption feature at line center. We find that the value of the Planck function representing the emission due to the wave in the dynamical model is about 30% of the value of the Planck function in the FAL model FALA. From the observations in Fig. 1

we estimated that the wave contributes only 5%. We attribute the larger value of 30% to the effect of geometry on wave propagation.

#### 4. Spherical wave propagation

The H line intensity in the CS model, which is too low to represent the emission of even the coolest FAL model and too high to represent the line emission alone suggests that the waves propagate not as plane waves but as 3D waves. That this must be the case is also evident from the comparison of the instantaneous values of the maximal  $H_{2v}$  emission in the simulations and in the observations of LRK93, which the model ought to match exactly since both are based on the same velocity spectrum or, rather, since there may be waves in the Sun which are not registered in observations that extend only to acoustic frequencies of about 10 mHz, the observed intensity is an upper limit for the simulated intensity. But the comparison displayed on the frontispiece of the proceedings volume of the Oslo conference (Carlsson 1994) shows that the simulated maximal intensity is much higher than the corresponding observed intensity. This discrepancy would be explained by spherical wave propagation, which allows the wave energy to spread horizontally as the wave propagates vertically (Kalkofen 2003).

The horizontal expansion of the upward-traveling wave energy can be seen in the filling factor of bright points, which is 5% to 10% in the middle chromosphere, where the emission peaks of the calcium lines are formed. At the top of the chromosphere, the SUMER observations reported by Carlsson, Judge & Wilhelm (1997) give a value of  $f = 0.5$  for the regions of enhanced emission in C, N and O lines. The filling factors suggest that the propagation channel of the waves expands upward and that the source of the waves lies in the upper photosphere.

A more detailed picture of the horizontal spread of the wave energy emerges from the variation of the diameter,  $d$ , of the region disturbed by the upward-propagating shock wave with height,  $z$ :

$z = 2$ Mm	$d \sim 5$ Mm	Carlsson, Judge & Wilhelm (1997)
$z = 1$ Mm	$d \sim 2$ Mm	Cram & Damé (1983)
$z = 0.5$ Mm	$d \sim 1$ Mm	Foing & Bonnet (1984)
$z \sim 0$	$d \sim 0.2$ Mm	Sivaraman, Bagare & November (1990)

The features whose sizes are given in the table have been measured with the SUMER instrument on the SOHO spacecraft (Carlsson et al. 1997), with ground-based telescopes (H line: Cram & Damé 1983; K line: Sivaraman et al. 1990) and in a rocket flight (1600 Å continuum: Foing & Bonnet 1984).

From the properties of wave propagation (Bodo et al. 2000) it is clear that the intensity enhancements generally line up vertically. Even though the features refer to different elements and transitions and the measurements have been made at different times we may view the dependence of the cross section of the disturbed area as defining a propagation cone whose horizontal cross section is given by  $d/2 \approx 0.1 + z$ . This describes a cone with an opening angle of  $90^\circ$ .

The bounding surface of the cone is an approximation, as shown by the analytic solution of the three-dimensional hydrodynamic equations for impulsive wave excitation by Bodo et al. (2000), where the variation of the pressure disturbance due to the waves varies only slowly with zenith angle and where,

furthermore, the angular variation of the pressure depends on the order of the oscillation in the wake of the pulse.

The propagation cone is defined by observations, which include calcium lines both at the origin, in intergranular lanes (from which we take the width as a measure of the diameter of the wave source) and in the middle chromosphere. The relation  $d(z)$  for the cone allows us to estimate its expansion between the height of formation of the Fe I line, whose Doppler motion provides the boundary condition in the dynamical model, and the height of formation of the H<sub>2v</sub> emission peak. With the height of  $z = 250$  km for Fe I given by LRK93 and the height of 1 Mm for calcium, the expansion of the cross sectional area of the cone is by a factor of 10.

If we reduce the estimated fractional contribution of the wave to (local) chromospheric heating by the area factor we arrive at a value of 3%, in good agreement (given the uncertainties of the procedure) with the estimate of 5% drawn from the observations of vUK95.

A plane wave and a spherical wave dissipate by different amounts. Since the shock amplitude is higher in the plane wave, part of the difference between the observed emission due to the wave and the corrected emission of the model is due to the higher dissipation. Adjusting the simulated emission for this effect goes in the direction of changing the corrected value of 3% upwards, which tends to reduce the difference between the observed and simulated contributions.

To summarize: We have explained the difference between the FAL and CS models as being due to the absence of background heating in the CS model and inflated wave amplification due to the treatment of the waves as plane.

## 5. Stellar chromospheres

It is commonly assumed in modeling chromospheric heating that the acoustic waves are plane and are emitted by a plane source. The experience with chromospheric oscillations suggests, however, that the waves are spherical and are emitted by distributed sources. If, as seems likely, the chromospheric oscillations display a universal property of wave propagation in a stratified atmosphere, a comparison of models and observations should reveal the difference, in which the modeled dissipation and, hence, the radiative emission of the plane waves in the low chromosphere is higher than observed. The excess dissipation reduces the acoustic energy flux in the wave, which arrives in the upper layers of the chromosphere with less energy. Our expectation is therefore that plane-wave models show higher emission than stars do for radiation emitted low in the chromosphere, and lower emission for radiation emitted high in the chromosphere.

As is expected from the difference between spherical waves and plane waves, the lower limit of the modeled calcium emission (shown dashed in Figure 3) is higher than the observed limit (shown as dots).

The analysis of the line profiles to determine the chromospheric part of the emission alone is difficult, and Fawzy et al. (2002) suggest that the discrepancy between models and stars is the fault of the observers. But our results from chromospheric oscillations suggest that the problem may lie with the geometrical properties of wave propagation.



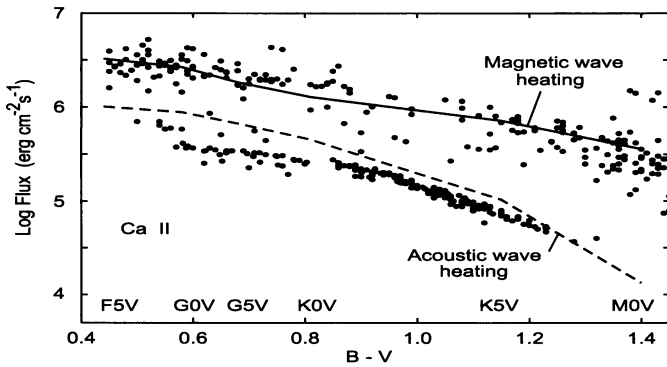


Figure 3. Chromospheric Ca II emission as a function of spectral class (Fawzy et al. 2002)

A similar comparison as the one shown in Fig. 3 but for emission in the Mg II lines, which are formed higher in the chromosphere, reveals that the models have less emission than is found in the stars. Fawzy et al. suggest that another heating mechanism supplies the energy missing from the models and propose microflares as the mechanism instead. But it seems more plausible that the problem can be solved by treating the waves in the heating as spherical waves emitted from distributed sources. We note in passing that this problem is more difficult to treat computationally than plane waves, which are already demanding in programming and computer resources.

## 6. Conclusions

Oscillations in calcium grains and the general chromospheric heating are independent phenomena. Dissipation in 3 min oscillations contributes  $\sim 5\%$  to heating at grain locations, and  $\sim 0.5\%$  overall.

Acoustic waves in the chromosphere of the Sun and, presumably generally in stratified media, propagate upward as spherical waves in cone-shaped channels with an opening angle of  $\sim 90^\circ$ .

The difference in emission between the coolest of the semiempirical FAL models and the semiempirical CS model is explained as the effect of two features of the CS model: (1) the absence of background chromospheric heating in the dynamical simulation and (2) the assumption of plane acoustic waves, which inflates the energy flux density by an area factor of  $\sim 10$  between the layer of formation of the Fe I line, whose Doppler motion serves to drive the waves in the simulation, and the layer of formation of the  $H_{2v}$  emission peak.

The difference between the modeled and observed emission in Ca II and Mg II of late-type stars may at least partly be due to the assumed plane-wave propagation in the models, which increases dissipation and emission in the lower chromosphere and reduces it in the upper chromosphere.

**Acknowledgments.** I thank Reiner Hammer for comments on the manuscript. I have enjoyed the hospitality of the Kiepenheuer Institut für Sonnenphysik and thank the University of Freiburg for a Mercator Professorship. I am also grateful to NASA for support to attend the IAU meeting in Australia.

## References

- Bodo, G., Kalkofen, W., Massaglia, S. & Rossi, P. 2000, *A&A*, 354, 296
- Brandt, P.N., Rutten, R.J., Shine, R.A., & Trujillo-Bueno, J. 1992, in *ASP Conf. Ser.*, Vol. 26, *Cambridge Workshop on Cool Stars, Stellar Systems, and the Sun*, M.S. Giampapa and J.A. Bookbinder eds., (San Francisco: ASP), 161
- Carlsson, M. 1994, in *Chromospheric Dynamics*, Proc. Mini-Workshop, Inst. Theor. Astroph., Oslo, frontispiece
- Carlsson, M., Judge, Ph., & Wilhelm, K. 1997, *ApJ*, 486, L63
- Carlsson, M. & Stein, R. F. 1994, in *Chromospheric Dynamics*, Proc. Mini-Workshop, Inst. Theor. Astroph., Oslo, 47 (CS)
- Carlsson, M. & Stein, R. F. 1995, *ApJ* 440, L29 (CS)
- Cram, L. E. & Damé, L. 1983, *ApJ*, 272, 355
- Damé, L., 1984, in: *Small-Scale Dynamical Processes in Quiet Stellar Chromospheres*, S. L. Keil ed., NSO/SPO, Sunspot, NM, 54
- Fawzy, D., Ulmschneider, P., Stepień, K., Musielak, Z.E., & Rammacher, W. 2002, *A&A*, 385, 983
- Foing, B. & Bonnet, R. M. 1984, *ApJ*, 279, 848
- Fontenla, J.M., Avrett, E.H., & Loeser, R. 1993, *ApJ*, 406, 319 (FAL)
- Kalkofen, W. 2003, *ASP Conf. Ser.*, 286, A.A. Pevtsov and H. Uitenbroek eds., 385
- Kariyappa, R. 1992, Thesis, Bangalore University
- Lites, B. W., Rutten, R. J. & Kalkofen, W. 1993, *ApJ*, 414, 345 (LRK93)
- Rutten, R.J. & Uitenbroek, H. 1991, *Sol. Phys.*, 134, 15
- Sivaraman, K.R., Bagare, S.P. & November, L.J. 1990, in *Basis Plasma Processes on the Sun*, Dordrecht: Kluwer, 102
- von Uexküll, M., & Kneer, F. 1995, *A&A*, 294, 252 (vUK95)